Nuclear Physics B244 (1984) 523–540

ANALYSIS OF COLEMAN-WEINBERG POTENTIALS IN ORBIT SPACE: GENERAL METHOD AND APPLICATION TO THE INFLATIONARY UNIVERSE

Jai Sam KIM*

Department of Physics, Washington University, St. Louis, MO 63130, USA

C.W. KIM

Department of Physics, Johns Hopkins University, Baltimore, MD 21218, USA

Received 1 November 1983
(Revised 27 March 1984)

We present a general method to analyze Coleman-Weinberg potentials in the orbit space, which is applicable to any irreducible representation. As an example, the structure of the SU(5) Coleman-Weinberg potential with scalars assigned to the adjoint representation is analyzed in complete detail, which confirms the general conclusion reached by Breit, Gupta and Zaks, and Moss that the phase transition in the new inflationary scenario of the early universe is problematic. We show that the disease found in the SU(5) case is common to all SU(N) ($N > 3$) and SO($2N$) ($N \neq 4, 8$) adjoints, and that the adjoints of SO(8) and exceptional groups are immune from the disease.

1. Introduction

Physical consequences of the grand unified theories depend sensitively on the detailed mechanisms of symmetry breaking as well as on the choice of scalar potentials that break the symmetry. For example, when the two well-known mechanisms of symmetry breaking, one due to explicit quadratic and/or cubic terms in the zero-loop effective potential (so-called Higgs mechanism) and the other due to radiative corrections (so-called Coleman-Weinberg mechanism [1]) are applied to the inflationary scenario of the very early universe, two entirely different pictures of the universe emerge. In the first case, which is the original Guth's model [2], the transition of the false vacuum to the stable $SU(3) \times SU(2) \times U(1)$ vacuum is strongly first order, leading to unacceptably excessive inhomogeneity.

On the other hand, the new inflationary model of Linde [3] and Albrecht and Steinhardt [4], which is based on the use of the Coleman-Weinberg potential,

* Present address: Department of Physics, Johns Hopkins University, Baltimore, MD 21218.

appears to provide a satisfactory phase transition from SU(5) to $SU(3) \times SU(2) \times U(1)$. Although the model has later been shown [5] to fail to produce the correct density fluctuation of $\delta\rho/\rho \sim 10^{-4}$, the flatness of the potential near the origin gives rise to the desired inflation enough to cure the horizon, flatness and monopole problems.

Recently, however, Breit, Gupta and Zaks [6] and Moss [7] have shown that the phase transition in the new inflationary model is problematic. They have observed that when represented by a diagonal 5×5 matrix instead of only one direction as done in previous analyses, the evolution of the Higgs fields is always through the $SU(4) \times U(1)$ local minimum for a reasonable range of the parameter b in the potential. When the Higgs fields get trapped in the $SU(4) \times U(1)$ minimum, the transition from the $SU(4) \times U(1)$ local minimum to the $SU(3) \times SU(2) \times U(1)$ minimum is again strongly first order as in the case of the original inflationary scenario, leading to the usual problem. When the fields do not get trapped in the $SU(4) \times U(1)$, they evolve towards the direction of the $SU(3) \times SU(2) \times U(1)$ minimum. In this case, new monopoles will be produced, leading perhaps to the monopole excess problem. However, Moss [7] has shown that, for certain ranges of the parameters in the potential, the present-day monopole density can be reduced to an acceptable level due to the quantum fluctuations of the Higgs fields.

A careful reexamination of the Coleman-Weinberg potential and an independent confirmation of the results obtained in refs. [6, 7] seem necessary. In this work, using the method [8] based on the orbit space and on the contour of the directional minimum, we present a fully detailed analysis of the Coleman-Weinberg potential, namely we investigate the absolute minimum, local extrema, ridges and valleys of the potential. We elaborate the general conclusion made in refs. [6, 7].

In sect. 2, we present a general method to analyze a general Coleman-Weinberg potential with one-loop radiative corrections in the orbit space. Prescriptions for finding the absolute minimum, local extrema and others are given. In sect. 3, the complete profile of the SU(5) Coleman-Weinberg potential with the adjoint representation is given as an example. In sect. 4 we summarize our results for the SU(5) adjoint. We show that the disease found in the SU(5) case is common to all $SU(N)$ $(N > 3)$ and $SO(2N)$ $(N \neq 4, 8)$ adjoints, and that the adjoints of SO(8) and exceptional groups are immune from the disease.

2. Analysis of Coleman-Weinberg potential

2.1. STRUCTURE OF AN EFFECTIVE POTENTIAL WITH ONE-LOOP RADIATIVE CORRECTIONS

For a massless non-abelian gauge field theory with the symmetry group G, the effective potential with one-loop radiative corrections was derived by Coleman and

Weinberg [1]:

$$V_{\text{eff}} = V_0 + V_s + V_g + V_f + V_c, \tag{1}$$

where V_0 is the classical 4th degree invariant polynomial, $V_s = (1/64\pi^2) \times \mathrm{Tr}[W^2(\phi_c)\ln W(\phi_c)]$ the contribution from the scalar loops, $V_g = (3/64\pi^2) \times \mathrm{Tr}[M^2(\phi_c)\ln M(\phi_c)]$ from the gauge boson loops, $V_f = (-1/64\pi^2) \times \mathrm{Tr}[(mm^\dagger)^2 \ln(mm^\dagger)]$ from the fermion loops, and V_c is the renormalization counterterm. The scalar and gauge boson mass matrices $W(\phi_c)$ and $M(\phi_c)$ are of second degree in ϕ_c, and the fermion mass matrix $m(\phi_c)$ is of first degree in ϕ_c.

2.2. GROUP THEORETICAL BACKGROUND

Despite its formidable appearance, the effective potential has a very simple structure. The Coleman-Weinberg potential including one-loop radiative corrections with the scalar assigned to an irreducible representation is always reduced to the following simple form (neglecting a coefficient with dimension $[M^4]$):

$$V_{\text{eff}} = \alpha r^4 \ln r^2 + \beta r^4, \tag{2}$$

where $r^2 = \|\phi\|/\mu^2$ and μ is the mass scale at the renormalization point. (α, β) contain all the directional information (their definitions may contain coupling constants, however). In other words (α, β) can be considered as generalized orbit parameters [8], specifying a direction in the representation space [9]. Formerly, we have used the dimensionless ratios of invariant polynomials for imaging the orbit space. Here we have introduced a non-polynomial invariant.

There are some subtleties in using non-polynomial invariant functions for representing the orbit space. Polynomial invariants provide a faithful image of a true orbit space because they neither smear out the singularities of the true orbit space nor introduce new singularities themselves. Some examples were given in refs. [10, 11]. Carefully selected smooth non-polynomial invariant functions can also provide a faithful image because they are smooth functions of polynomial invariants [12]. However, indiscriminate choice may introduce additional singularities or may even alter the topological structure. As we shall see, our analysis is useful even for those badly chosen functions that we may have to deal with in physics.

2.3. FINDING THE ABSOLUTE MINIMUM

The procedure that has been used previously [8] to analyze the classical fourth degree polynomial potential can be used to find the absolute minimum of the potential in eq. (1).

Along a given direction specified by (α, β), the potential has a directional maximum at the origin and a directional minimum at $r_0(\alpha, \beta)$ which is given by

$$r_0^2 = \exp\left(-\frac{\beta}{\alpha} - \tfrac{1}{2}\right), \tag{3}$$

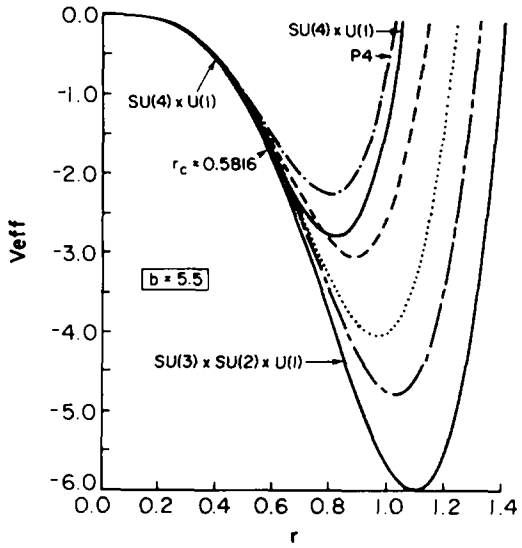

Fig. 1. The profile of the SU(5) Coleman-Weinberg potential given by eqs. (2), (7) at $b = 5.5$ along various directions.

with the potential value

$$V_{\text{eff},0} = -\tfrac{1}{2}\alpha \exp\left(-\frac{2\beta}{\alpha} - 1\right) \equiv k\,. \tag{4}$$

The behavior of the potential is illustrated in fig. 1. Eq. (4) can be solved for β:

$$\beta = -\tfrac{1}{2}\alpha\left[\ln\left(-\frac{2k}{\alpha}\right) + 1\right]. \tag{5}$$

The contour of directional minima given by eq. (5) is plotted in fig. 2 in the first and fourth quadrants. It is antisymmetric with respect to the origin.

The absolute minimum occurs at the point where the contour makes the first contact with the orbit space as we increase the k value from $-\infty$.

The contour given by eq. (5) is universal to any irreducible representations to which the scalar fields are assigned. Different representations have different orbit spaces and little groups.

2.4. ANALYZING THE EXTREMUM STRUCTURE

As we have shown in ref. [10], our method also reveals the extremum structure of the potential. The rule is that there is an extremum at:

(i) every cusp;

(ii) a point on the orbit space boundary which contacts the contour of directional extremum tangentially.

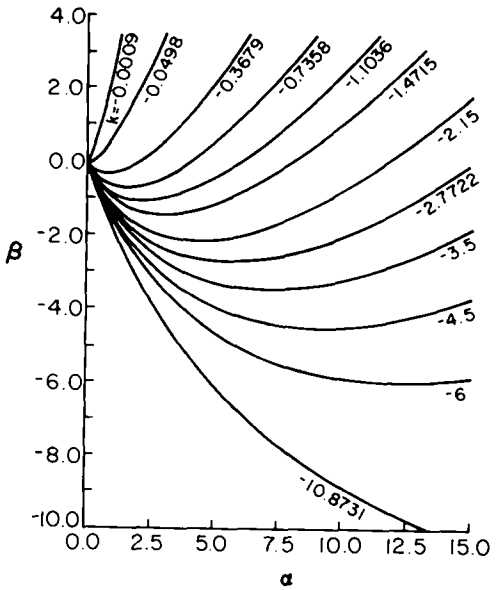

Fig. 2. Contour of the directional minimum given by eq. (5).

The rules concerning the nature of the extremum are:

(i) an extremum is a local extremum if it is the only local contact point when the contour enters into the orbit space locally, fig. 3a;

(ii) an extremum is a saddle-point if it is the only local contact point when the contour leaves the orbit space locally, fig. 3b;

(iii) an extremum is an inflection point if there is a continuum of neighboring points meeting the contour, fig. 3c.

In our convention, the contour moves in the direction of increasing equipotential for the local minimum, and in the equipotential decreasing direction for the local maximum.

2.5. ANALYZING THE PROFILE

Suppose we want to know the structure of the potential at a given radius r and direction (α, β). Eq. (2) provides the value of the potential in a simple and straightforward way. We can analyze the cross section of the potential at any radius. For fixed r, it is simply an equation of a straight line with a fixed slope $d\beta/d\alpha = -\ln r^2$. Thus the problem reduces to that of finding which part of the orbit space gets the first contact as we increase k_ℓ defined by

$$\alpha r^4 \ln r^2 + \beta r^4 \equiv k_\ell . \tag{6}$$

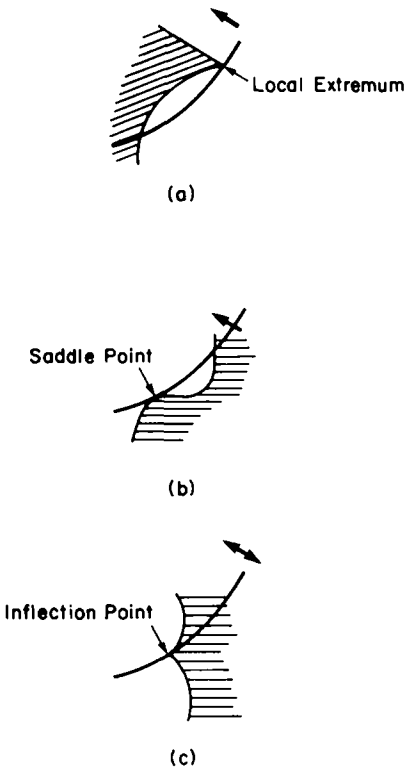

Fig. 3. The nature of local extrema depends on the environment of the orbit-space boundary point making contact with the contour. (a) Contour enters into the orbit space at a locally isolated point – local extremum. (b) Contour leaves locally the orbit space – local saddle-point. (c) Contour meets a continuum of points – an inflection-point.

For $r^2 < 1$, $d\beta/d\alpha > 0$ and the line moves to the upper-left direction as k_ℓ increases. For $r^2 > 1$, $d\beta/d\alpha < 0$ and the line moves to the upper-right direction as k_ℓ increases.

This simple approach provides us with the detailed information about the structure of the potential, as will be demonstrated in the following section.

Before we proceed to discuss an example, we make a few additional comments on the general method. In general, one-loop corrections from scalars, gauge bosons and fermions all have different structures. Thus, β in eq. (2) should be replaced by $\beta_s + \beta_g + \beta_f$. Also, when there are many algebraically independent fourth degree invariants, eq. (2) includes $\alpha_1, \alpha_2, \ldots$ (β may contain additional orbit parameters that are not in α). In this case, the dimension of the orbit space in eq. (2) can be higher than two or even higher than that of the true orbit space (in this case there are constraints among α's and β's). If one is interested only in the absolute minimum, then eq. (2) with (α, β) is sufficient. However, if one wants to know the extremum

structure and the profile, eq. (2) should be equipped with $(\alpha_1, \alpha_2, \ldots; \beta_s, \beta_g, \beta_f)$. Otherwise, extremum points found in the $(\alpha_1, \alpha_2, \ldots; \beta_s, \beta_g, \beta_f)$ space can be buried [10] in the (α, β) space.

For physical reasons, β_s and β_f are normally suppressed in the one-loop approximation. For the adjoint representations of most classical Lie groups eq. (2) has only one nontrivial α. The adjoint representations of SO(4), SO(8), SU(3), and all the exceptional groups do not yield nontrivial α. The SO(8) adjoint contains three independent orbit parameters in β, however.

3. Example: adjoint representation of SU(5)

In this section we consider, as an example, the Coleman-Weinberg potential where the scalar fields transform as the adjoint representation of SU(5). This has often been used to study the structure of the grand unified theories and their physical implications. The new inflationary scenario of the early universe was indeed based on the SU(5) model with the Coleman-Weinberg potential. In view of the importance of the recent works by Breit et al. [6], and Moss [7] in deciding the fate of the new inflationary model, it deserves a careful reexamination. It also serves as an interesting illustrative example of our general method.

Although the method described in the previous section can be applied to more complicated cases where all the one-loop radiative correction terms V_s, V_g and V_f are included, we discuss the simplest case where only V_g is included. Also, the renormalization prescription can be given in a simple and intuitive way in the orbit space. In this section we concentrate on the illustration of our method and the confirmation of the conclusions made in refs. [6, 7].

We employ exactly the same form for the effective potential as in ref. [6]:

$$V_{\text{eff}} = \frac{3g^4}{256\pi^2}\left\{ b\left[\sum_{i=1}^{5} a_i^4 - \tfrac{7}{30}\left(\sum_{i=1}^{5} a_i^2 \right)^2 \right] + \sum_{i,j=1}^{5} (a_i - a_j)^4 \left[\ln\left(\frac{a_i - a_j}{\mu} \right)^2 - \tfrac{1}{2} \right] \right\}, \tag{7}$$

with

$$\sum_{i=1}^{5} a_i = 0 .$$

Comparing eqs. (2) and (7), we find that

$$\alpha = \sum_{i,j=1}^{5} (A_i - A_j)^4 / r^4, \tag{8}$$

$$\beta = \sum_{i,j=1}^{5} \left\{ \frac{(A_i - A_j)^4}{r^4} \ln\left[\frac{(A_i - A_j)^2}{r^2} \right] \right\} - \tfrac{1}{2} \sum_{i,j=1}^{5} \frac{(A_i - A_j)^4}{r^4} + b \left(\frac{\sum_{i=1}^{5} A_i^4}{r^4} - \tfrac{7}{30} \right), \tag{9}$$

where $A_i = a_i/\mu$ and $r^2 = \Sigma_{i=1}^{5} A_i^2$.

The overall factor $(3g^4/256\pi^2)$ has no significance in our analysis. (This factor may be absorbed in the definition of α and β.)

The orbit space (α, β) is plotted in fig. 4 with $b = 5.5$. Its evolution with b is shown in fig. 5. In obtaining this, we have used the same method as in refs. [8,10]; namely by substituting the singlet forms for successively low-level little groups into eqs. (8) and (9). The little groups and singlet forms are given in table 1.

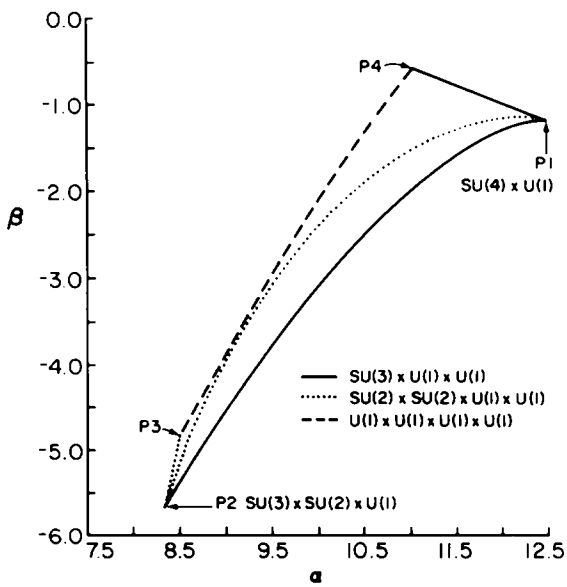

Fig. 4. The orbit space of the SU(5) adjoint representation given by eqs. (8), (9) at $b = 5.5$. The singlet forms are given in table 1. The solid, dotted, and dashed lines are, respectively, for $SU(3) \times U(1) \times U(1)$, $SU(2) \times SU(2) \times U(1) \times U(1)$, and $U(1) \times U(1) \times U(1) \times U(1)$.

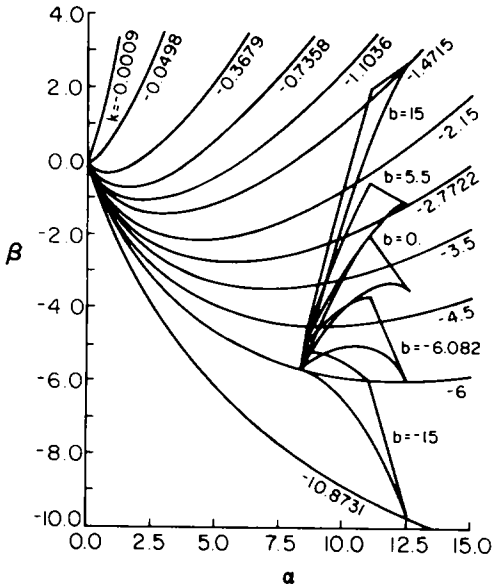

Fig. 5. The evolution of the orbit space with b laid over the contour of directional minimum contains all the necessary information needed to determine the absolute minimum, local extrema and the profile of the Coleman-Weinberg potential.

There are two cusps of maximum little groups P1 and P2 and most of the boundaries P4 → P1 → P2 → P3 correspond to semi-maximal little groups, which is the general property of a true orbit space. However, the boundary is not fully closed by higher level little groups. The boundary portion P3–P4 corresponds to the lowest-level little group $U(1)\times U(1)\times U(1)\times U(1)$ and is convex. Also unexpected cusps at P3 and P4 have appeared. This is in contrast to the faithful orbit-space image constructed from polynomial invariants. The logarithmic functions have introduced their own singularities and changed the topological structure of the true

TABLE 1
Singlet forms for little groups for the orbit space boundary

	Little groups	Singlet forms
P1	$SU(4)\times U(1)$	$a[1,1,1,1,-4]$
P2	$SU(3)\times SU(2)\times U(1)$	$a[1,1,1,-\frac{3}{2},-\frac{3}{2}]$
P3	$SU(2)\times SU(2)\times U(1)\times U(1)$	$a[1,1,-1,-1,0]$
P4	$SU(3)\times U(1)\times U(1)$	$a[1,-1,0,0,0]$
P4–P1–P2	$SU(3)\times U(1)\times U(1)$	$a[1,1,1,t,-3-t]$
P1–P2–P3	$SU(2)\times SU(2)\times U(1)\times U(1)$	$a[1,1,t,t,-2-2t]$
P3–P4	$U(1)\times U(1)\times U(1)\times U(1)$	$a[1,-1,t,\ t,0]$

orbit space. It is noteworthy that the boundary portion of P1–P4 is not a straight line but a concave curve as the curves P1–P2 and P2–P3 are.

3.1. THE ABSOLUTE MINIMUM

Since the contour of directional minimum is concave in the direction of increasing equipotential k and the strata of $SU(3)\times SU(2)\times U(1)$ and $SU(4)\times U(1)$ are most protrudent towards this direction, the absolute minimum occurs only at one of these two points.

First we note that the contour of directional minima, eq. (5), meets P1 and P2 simultaneously at $b = b_c$:

$$b_c = -15\ln\tfrac{3}{2} = -6.082. \tag{10}$$

Therefore, for $b > b_c$, the absolute minimum occurs at the orbit of $SU(3)\times SU(2)\times U(1)$ with

$$\begin{aligned} r_0^2 &= \tfrac{6}{5}, \qquad V_{\mathrm{eff},0} = -6, \\ \alpha(\mathrm{P2}) &= \tfrac{25}{3} \\ \beta(\mathrm{P2}) &= \tfrac{25}{3}\ln\tfrac{5}{6} - \tfrac{25}{6}, \end{aligned} \tag{11}$$

and for $b < b_c$, the absolute minimum occurs at the orbit of $SU(4)\times U(1)$ with

$$\begin{aligned} r_0^2 &= \tfrac{4}{5}e^{-b/30}, \qquad V_{\mathrm{eff},0} = -4e^{-b/15}, \\ \alpha(\mathrm{P1}) &= \tfrac{25}{2}, \\ \beta(\mathrm{P1}) &= -\tfrac{25}{4} + \tfrac{5}{12}b + \tfrac{25}{2}\ln\tfrac{5}{4}. \end{aligned} \tag{12}$$

For future reference, we give the values of α and β for P3 and P4:

$$\alpha(\mathrm{P3}) = \tfrac{17}{2}, \qquad \beta(\mathrm{P3}) = -\tfrac{17}{4} - \ln 2 + \tfrac{1}{60}b, \tag{13}$$

$$\alpha(\mathrm{P4}) = 11, \qquad \beta(\mathrm{P4}) = -\tfrac{11}{2} + 5\ln 2 + \tfrac{4}{15}b. \tag{14}$$

3.2. THE EXTREMUM STRUCTURE

The extremum structure of the potential (7) is rather complicated and depends sensitively on b. We will show it for each different range of b in fig. 5.

The behavior of P1 and P2 as a function of b is rather simple. P1 is a saddle-point for $b \geqslant b_u = 15$ and a local minimum for $b < 15$. P2 is a local minimum for $b > b_d = -15$, an inflection point for $-15 \geqslant b > b_\ell$, and the saddle-point for $b \leqslant b_\ell = -60[\tfrac{17}{4}\ln\tfrac{24}{17} - \ln 2] = -46.35$.

For $b > b_h$, where $b_h = 55[\frac{10}{11}\ln 2 - \ln\frac{11}{8}] = 17.142$, P3 and P4 are both inflection points and there are no additional extrema. At $b = b_h$, $V_{\mathrm{eff},0}(\mathrm{P4}) = V_{\mathrm{eff},0}(\mathrm{P1})$. For $b_h > b > b_u$, P4 becomes the global saddle point with P3 remaining an inflection point. At $b = b_u$, the contour meets P1 tangentially. The b_u is obtained by equating the slope of the contour at P1

$$\left[\frac{\mathrm{d}\beta}{\mathrm{d}\alpha}\right]_{\mathrm{contour}} = \frac{\beta}{\alpha} + \tfrac{1}{2} = \ln\tfrac{5}{4} + \tfrac{1}{30}b \quad \text{at P1}, \tag{15}$$

with the slope of the orbit space boundary at P1

$$\left[\frac{\mathrm{d}\beta}{\mathrm{d}t} \Big/ \frac{\mathrm{d}\alpha}{\mathrm{d}t}\right]_{t=1} = -1 + \ln\tfrac{5}{4} + \tfrac{1}{10}b. \tag{16}$$

As b is lowered from b_u, a new inflection point appears from P1 on the curve P1–P2, moves towards P2, and arrives at P2 at $b = b_d = -15$ where the contour meets P2 tangentially (to the curve P1–P2). The b_d is obtained from

$$\left[\frac{\mathrm{d}\beta}{\mathrm{d}\alpha}\right]_{\mathrm{contour}} = \left[\frac{\mathrm{d}\beta}{\mathrm{d}t} \Big/ \frac{\mathrm{d}\alpha}{\mathrm{d}t}\right]_{t=\ 1.5} \quad \text{at P2}, \tag{17}$$

or

$$\ln\tfrac{5}{6} = \tfrac{3}{2} + \ln\tfrac{5}{6} + \tfrac{1}{10}b. \tag{18}$$

As b is lowered from b_u, P4 remains the saddle-point until the contour meets P4 tangentially (to the curve P4–P3) at $b = b_1$. For $b < b_1$, P4 is an inflection-point and a new saddle-point appears from P4 on the curve P4–P3, moves towards P3 and arrives at P3 at $b = b_2$, where the contour meets P3 tangentially (to the curve P4–P3). The b_1 and b_2 can be computed from equations similar to eq. (17).

For $b < b_2$, P3 remains a saddle-point until the contour passes P2 and P3 simultaneously at $b = b_\ell$. For $b < b_\ell$, P3 is an inflection point and P2 is the saddle-point.

From eq. (3) we can compute r_0 for P1 and P2 and the value of $b(\equiv b_r)$ when $r_0(\mathrm{P1}) = r_0(\mathrm{P2})$. The b_r is obtained from

$$r_0(\mathrm{P1}) = [\mathrm{e}^{\ \beta/\alpha - 1/2}]_{\mathrm{P1}} = r_0(\mathrm{P2}) = [\mathrm{e}^{\ \beta/\alpha - 1/2}]_{\mathrm{P2}}, \tag{19}$$

which yields

$$b_r = -30\ln\tfrac{3}{2} = -12.164. \tag{20}$$

For $b > b_r$, $r_0(\mathrm{P2})$ is greater than $r_0(\mathrm{P1})$ and for $b < b_r$, $r_0(\mathrm{P2})$ is the smaller.

3.3. THE PROFILE

Now we discuss the structure of ridges and valleys of the potential. The height of the potential at any radius r and direction (α, β) is given by

$$V_{\text{eff}} = \alpha r^4 \ln r^2 + \beta r^4 \equiv k_\ell . \tag{6}$$

For fixed r, eq. (6) is an equation of a straight line with the slope $s = \mathrm{d}\beta/\mathrm{d}\alpha = -\ln r^2$.

Near the origin s is large and positive. As k_ℓ increases, the line moves to the upper-left direction. P1 gets the first contact and P2 the last. Thus the orbit of $SU(4) \times U(1)$ has the smallest potential value at a fixed radius near the origin and that of $SU(3) \times SU(2) \times U(1)$ the largest.

In order to elucidate, we shall consider the two regions of b separately: (i) $b > b_e$, and (ii) $b < b_e$, where

$$b_e = 5(2 \ln \tfrac{16}{45} + 1) = -5.341 \tag{21}$$

is the value of b where $\beta(\mathrm{P1}) = \beta(\mathrm{P2})$. In the region (i) $(b > b_e)$ the orbit space is tilted to the upper-right direction. As r increases, s decreases and at $r = r_c$, P1 and P2 have the same potential value. The r_c is found from

$$-\ln r_c^2 = \frac{\beta(\mathrm{P1}) - \beta(\mathrm{P2})}{\alpha(\mathrm{P1}) - \alpha(\mathrm{P2})} , \tag{22}$$

which reduces to

$$r_c^2 = \tfrac{16}{45} \exp\left(\tfrac{1}{2} - \tfrac{1}{10} b\right) . \tag{23}$$

Between $r_c < r < 1$, P2 remains the first contact point. As r passes 1, s becomes negative. For $r > 1$, the line moves to the upper-right direction as k_ℓ increases. One can easily see that P2 is always the first contact point.

In the region (ii) $(b < b_e)$ the orbit space is tilted to the lower-right direction. Again the potential value of P1 is the smallest near the origin. As r passes 1, the potential value of P1 remains the smallest. As r reaches r_c (which is greater than 1 for $b < b_e$), P2 becomes the smallest and remains that way.

Thus either P1 or P2 is the smallest at any radius r for any value of b. The profile of the potential for different values of b is illustrated in fig. 6. However, this does not mean that, using the classical picture of a ball (or bubble) rolling down the potential hill, a ball released at the origin rolls down along the $SU(4) \times U(1)$ valley and at $r = r_c$ jumps down to the $SU(3) \times SU(2) \times U(1)$ valley, for there is a high ridge between the two valleys.

Let us check if there is a hidden trail leading from P1 to P2. Just beyond r_c, a typical situation is as shown in fig. 7. Since the curve P1–P2 is concave, the point P1

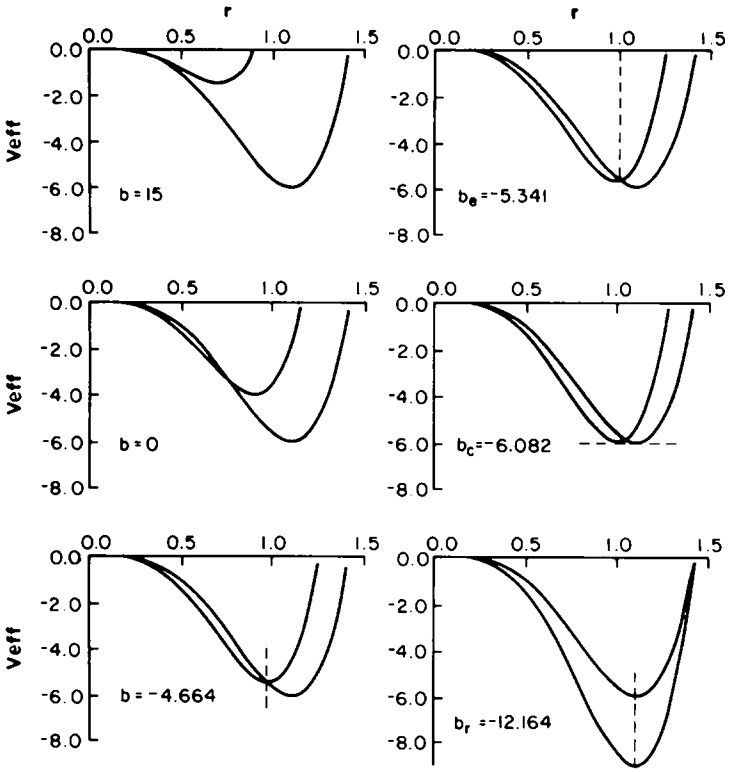

Fig. 6. (a) The profile of the potential along the $SU(3) \times SU(2) \times U(1)$ and $SU(4) \times U(1)$ directions at various b. The curve with the minimum value, -6, is the $SU(3) \times SU(2) \times U(1)$ profile.

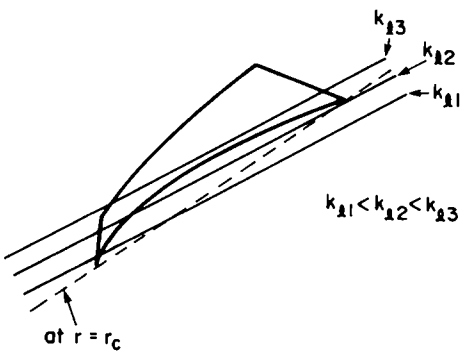

Fig. 7. The height and local property of the potential at a given radius are determined by eq. (6).

is isolated from its neighbor when it meets the line. This means that P1 is truly a local valley. However, as r increases, the line tilts clockwise until it can meet P1 tangentially. Here one finds a hidden trail leading to P2. The radius at which this happens is found from

$$-\ln r_t^2 = \left[\left(\frac{d\beta}{dt}\right)\Big/\left(\frac{d\alpha}{dt}\right)\right]_{t=1},$$

or

$$r_t^2 = \tfrac{4}{5}e^{1-b/10}. \tag{24}$$

As r increases further, the line keeps on rotating until it can meet P4 and P1 simultaneously. This happens at

$$-\ln r_s^2 = \frac{\beta(\mathrm{P1})-\beta(\mathrm{P4})}{\alpha(\mathrm{P1})-\alpha(\mathrm{P4})},$$

or

$$r_s^2 = \exp\left[-\tfrac{1}{10}b + 20\ln 2 - \tfrac{25}{3}\ln 5 + \tfrac{1}{2}\right]. \tag{25}$$

Beyond r_s, the SU(4) × U(1) direction emerges as the globally highest ridge.

If the effective potential value is negative at $r^2 = r_t^2$, then the ball released at the origin has enough energy to climb up the hill to reach the hidden trail (neglecting any energy loss due to possible frictions). The lower bound on b for this to happen is given by

$$V_{\mathrm{eff}} = 0 = \alpha(\mathrm{P1})r_t^4 \ln r_t^2 + \beta(\mathrm{P1})r_t^4,$$

or

$$b = b_t = \tfrac{15}{2}. \tag{26}$$

For b larger than b_t, the ball starting from the origin rolls down the SU(4) × U(1) valley, climbs up the hill, comes out of the valley, and finally rolls down into the SU(3) × SU(2) × U(1) bottom. As b approaches b_u, r_t approaches $r_0(\mathrm{P1})$ and the two become identical at $b = b_u$. This is as expected since at $b = b_u$ the SU(4) × U(1) minimum becomes an inflection point.

4. Summary and conclusion

First we summarize the profile of the Coleman-Weinberg potential (without finite temperature corrections) as a function of the dimensionless parameter b by using the classical picture of a ball (or bubble) rolling down the potential hill.

4.1. $b > b_u (= 15)$

The bubble starts to roll down very slowly (this is the reason for inflation in the new inflationary scenario) along the SU(4) × U(1) valley, and accelerates down the valley until the valley ends somewhere (at $r = r_t$) on the slope before the saddle-point. After passing through the SU(4) × U(1) valley, it keeps rolling down fast towards the direction of the SU(3) × SU(2) × U(1).

4.2. $b_u (= 15) > b > b_t (= 7.5)$

Now the SU(4) × U(1) is a local minimum but the SU(3) × SU(2) × U(1) remains the absolute minimum. The former is closer to the origin than the latter. In this case, however, the bubble that is rolling down towards the SU(4) × U(1) minimum will not become trapped at the bottom of the SU(4) × U(1) valley but instead climbs up a ridge between the SU(4) × U(1) and SU(3) × SU(2) × U(1) valleys and rolls down to the SU(3) × SU(2) × U(1) minimum.

4.3. $b_t (= 7.5) > b > b_c (= -6.082)$

In this case, the general picture is the same as above except that the ridge becomes too high for the bubble to climb up so that the bubble will become trapped in the SU(4) × U(1) phase. The transition to the SU(3) × SU(2) × U(1) is then strongly first order.

4.4. $b_c (= -6.082) > b > b_r (= -12.164)$

The SU(4) × U(1) is now the absolute minimum and the bubble will not reach the SU(3) × SU(2) × U(1) minimum.

4.5 $b_r (= -12.164) > b > b_d (= -15)$

Now the SU(3) × SU(2) × U(1) minimum is closer to the origin than that of the SU(4) × U(1), but there is no valley leading directly to the SU(3) × SU(2) × U(1). The bubble will become trapped in the SU(4) × U(1) phase.

4.6. $b < b_d (= -15)$

The SU(4) × U(1) remains the absolute minimum but the SU(3) × SU(2) × U(1) is now an inflection-point, with no chance of the bubble ending up in the SU(3) × SU(2) × U(1) phase.

The profile of the potential described above agrees with the general picture obtained in refs. [6, 7]. However, the changes of the potential behavior at b_r, b_d and b_ℓ have not been mentioned in ref. [6] whereas none of b_t, b_r, b_d and b_ℓ was discussed in ref. [7]. In contrast to ref. [6], second derivatives need not be checked in our analysis.

So far we have described the profile of the potential by using a classical picture of a bubble rolling down the potential hill. However, in applying the results to the

inflationary scenario of the early universe, we must take the expansion of the universe into account. The expansion, which is exponential during the initial rolling stage, acts as frictions in the evolution equation of the Higgs fields and changes the value of $b_t = 7.5$ to $b_t' = 14.5$, as pointed out in ref. [6]. Therefore, cosmologically, the case of $b < b_t'(= 14.5)$ seems to be unacceptable since the phase transition to the $SU(3) \times SU(2) \times U(1)$ is either impossible or strongly first order. For $b > b_t'$, the bubble will eventually end up, in the absence of other frictions, in the $SU(3) \times SU(2) \times U(1)$ phase and due to the flatness of the potential near the origin, there will be enough inflation to solve the horizon and flatness problems. (We wish to point out that Breit et al. [6] have estimated the upper limit $b_{max} = 10$ to keep the one-loop correction due to the Higgs fields less than 10% of the usual terms.) However, when the bubble passes through the $SU(4) \times U(1)$ phase, which is inevitable, additional monopoles [7] may be produced. These monopoles cannot be sufficiently diluted by the inflation, leading to the monopole excess problem.

It should also be pointed out that in the cosmological analysis of the evolution of the Higgs fields, the temperature dependence of α and β through the gauge coupling constant g must be taken into account. Moreover, some frictions may appear due to the radiation energy loss by the Higgs fields. The quantum fluctuations can also modify the motion of the bubble. In fact, Moss [7] has shown that the quantum fluctuations may reduce, for some ranges of the parameters in the potential, the present-day monopole density considerably, even to an acceptably low level so as not to overclose the universe.

A word of caution is in order as for the region of validity of the Coleman-Weinberg potential. Although our analysis is accurate for a given potential, the Coleman-Weinberg potential is most reliable near the renormalization point. As r deviates far from r_0(P2), $|\ln r^2|$ becomes large and the one-loop approximation becomes meaningless. Eventually, the whole perturbation calculation breaks down. Thus our results are reliable only within a reasonable distance from $r = \sqrt{1.2}$. This leads to the following interesting possibility. If we tune the parameter b such that P2 is already the lowest at a distance r where the Coleman-Weinberg potential with one-loop corrections is valid, then the ball coming out of the unknown region of small r is likely to roll down the valley of P2. This is achieved by moving r_c near the origin as close as possible. In this case, the ball is more likely to fall into the P2 side of the ridge then into the P1 side because there are more directions available on the P2 side. If r_c were pushed into the fluctuation region arising from the finite Hawking temperature, this would certainly be the case. However, small r_c requires high $b(\simeq 10^2)$ and then multi-loop corrections should be considered. Detailed analysis [13] of the renormalization group equation prompted the necessity of multi-loop corrections.

The important characteristic of the SU(5) adjoint is that the $SU(3) \times SU(2) \times U(1)$ valley is not the lowest from the origin all the way down to the minimum point, contrary to what one has hoped for the success of the new inflationary model. This

disease found in the SU(5) case is common to all SU(N) ($N > 3$) and SO($2N$) ($N > 4$) adjoints because their orbit spaces are all alike. From eq. (2), one sees that as $r \to 0$, $\ln r^2$ goes to $-\infty$ and the orbit with the largest α yields the lowest potential value at a given radius near the origin. We have computed α generically for the two physically interesting groups: SU(N) and SO($2N$). $\alpha \propto (2N-5)\lambda_4 + 3$ for SU(N) adjoint ($N > 3$) with $\lambda_4 = \mathrm{Tr}\phi^4/(\mathrm{Tr}\phi^2)^2$, and $\alpha \propto (2N-8)\lambda_4 + 6$ for SO($2N$) adjoint ($N \geqslant 3$) with λ_4 defined similarly. From this and the tables given in ref. [8, 10], we find that in the case of SU(N) adjoints the largest α comes from the origin of SU($N-1$) $\times$ U(1) and the smallest α from SU[$\frac{1}{2}(N+1)$] $\times$ SU[$\frac{1}{2}(N-1)$] $\times$ U(1) [N: odd] and SU($\frac{1}{2}N$) $\times$ SU($\frac{1}{2}N$) $\times$ U(1) [N: even]. For SO($2N$) adjoints with $N > 4$, the largest α comes from SO($2N-2$) $\times$ U(1) and the smallest α from SU(N) $\times$ U(1). For the SO(8) adjoint, α is direction independent. The two independent quartic coupling constants related to $\mathrm{Tr}\phi^4$ and $\phi_1\phi_2\phi_3\phi_4$ are unaffected by the redefinition of renormalization point μ. In this case, the crossover does not occur and the potential has the lowest profile along the direction where the absolute minimum lies, which is determined by the two coupling constants.

The adjoints of exceptional groups are truly exceptional. Since there are no independent quartic invariants, only the β-term is direction dependent. One can immediately see that the potential is the lowest from the origin to the minimum point along the direction of the maximal little group that yields the smallest β. The only quartic coupling constant is absorbed in the redefinition of μ and there is no free parameter such as b. Thus the adjoints of exceptional groups do not allow us any control over the symmetry breaking directions. The absolute minima of the adjoints of exceptional groups have been found numerically in ref. [14].

The authors would like to thank Professor P. Steinhardt for useful discussions. One of the authors (J.S.K.) would like to thank Professors C.M. Bender and J.E. Mandula for their warm hospitality extended to him at Washington University. This research was supported in part by the Department of Energy and the National Science Foundation.

References

[1] S. Coleman and E. Weinberg, Phys. Rev. D7 (1973) 1888
[2] A.H. Guth, Phys. Rev. D23 (1981) 347
[3] A.D. Linde, Phys. Lett. 108B (1982) 389
[4] A. Albrecht and P. Steinhardt, Phys. Rev. Lett. 48 (1982) 1220;
S.W. Hawking and I.G. Moss, Phys. Lett. 110B (1982) 35
[5] S.W. Hawking, Phys. Lett. 115B (1982) 295;
A. Guth and S.-Y. Pi, Phys. Rev. Lett. 49 (1982) 1110;
J. Bardeen, P.J. Steinhardt and M.S. Turner, Phys. Rev. D28 (1983) 679
[6] J.D. Breit, S. Gupta and A. Zaks, Phys. Rev. Lett. 51 (1983) 1007
[7] I.G. Moss, Phys. Lett. 128B (1983) 385
[8] J. S. Kim, Nucl. Phys. B196 (1982) 285;
S. Frautschi and J.S. Kim, Nucl. Phys. B196 (1982) 301;
J.S. Kim, Nucl. Phys. B197 (1982) 174

[9] L. O'Raifeartaigh, Rep. Prog. Phys. 42 (1979) 159;
L. Michel, Rev. Mod. Phys. 52 (1980) 617
[10] J.S. Kim, J. Math. Phys. 25 (1984) 1694
[11] M. Abud and G. Sartori, Phys. Lett. 104B (1981) 147;
G. Sartori, J. Math. Phys. 24 (1983) 765;
M. Abud and G. Sartori, Ann. of Phys. 150 (1983) 307
[12] G.W. Schwarz, Topology, 14 (1975) 63
[13] M. Sher, Phys. Lett. 135B (1984) 52
[14] J. Harvey, Nucl. Phys. B163 (1980) 254